Analysis of Ionized Field under HVDC Transmission Lines within the Influences of Suspended Particles

Yan Li[1, 2], Shun Yuan[1], Fan Yang[3], Bing Gao[3], Tingting He[3, *], and Jia Ran[3]

Abstract—The ionized field under HVDC transmission lines have an impact on environment and people. With the industrial pollution and environment deterioration, the suspended particles that will influence the ionized field cannot be ignored. So the improved meshless local Petrov-Galerkin (MLPG) method, which can avoid the interpolation of boundary points is applied in this paper to calculate the ionized field of unipolar transmission line. Based on the calculation, the analysis of the ionized field within the influences of suspended particles has been done by establishing the charging model of suspended particles. The research shows that suspended particles indeed influence the ionized field by increasing space charge density, reducing corona onset electric field, and reducing the ion mobility.

1. INTRODUCTION

Compared with high-voltage alternating current (HVAC) power transmission, high-voltage direct current (HVDC) power transmission has more advantages such as lower electric losses, longer transmission distance, and bigger transmission capacity. However, the problems that HVDC power transmission generates cannot be concealed. The influences of the ionized field under HVDC transmission lines on environment and people cannot be ignored. So it is necessary to calculate and analyze the ionized field under HVDC transmission lines.

When the electric field strength on the surface of the conductors exceeds the onset value, there will be a layer of c around the conductor. The ions ionized in this corona layer and the charged suspended particles will distribute in the whole space around the conductors by the effect of diffusion and electric force, and then constitute a stable distribution of space charge. The coupling between the electric field and space charge makes the system nonlinear. A lot of researches have been done to characterize the ionized field with the influences of wind, sub-conductor number, line arrangements, and height of the conductors [1–3].

In the past decades, researchers have developed many calculation methods based on Deutsch assumption or Kaptzov assumption such as charge simulation method, method of moments, and finite element method (FEM). The FEM is widely used because of higher accuracy, efficiency, and flexibility among all these methods [4]. Janischewskyj and Gela [5], Takuma et al. [6], etc. have gotten a fine result by applying the FEM on the analysis of the ionized field under HVDC transmission lines.

The development of meshless method in electromagnetic calculation provides the theory and basis for the calculation of the ionized field under HVDC transmission lines [7, 8]. Compared with the FEM, the meshless method does not require the connection information of nodes [6]. Ref. [9] first utilized the MLPG method based on radial point interpolation shape function in the calculation of the ionized field under HVDC transmission lines. In practical terms, there will be a lot of suspended particles in the

air because of the industrial pollution and environment deterioration. The charging of these suspended particles will have a strong impact on the ionized field under HVDC transmission lines. Therefore, this paper proposes an improved MLPG method to calculate the ionized field of transmission lines within the influence of suspended particles. In Section 2, the improved MLPG method is proposed to calculate the ionized field, and the validation of the method is verified. In Section 3, the ionized field of unipolar HVDC transmission line is calculated to explore the influence of suspended particles. Finally, Section 4 concludes this paper.

2. THE CALCULATION OF IONIZED FIELD BASED ON IMPROVED MLPG METHOD

2.1. The Improved MLPG Method for Ionized Field

For the HVDC transmission lines with the effect of wind, the equations used for unipolar field are as follows [10–12]:

$$\nabla^2 \varphi = (\rho_- - \rho_+) / \varepsilon \tag{1}$$

$$\mathbf{E}_s = -\nabla \varphi \tag{2}$$

$$\mathbf{j} = \rho (K\mathbf{E} + \mathbf{w}) \tag{3}$$

$$\nabla \cdot \mathbf{j} = 0 \tag{4}$$

where the subscripts $+$ and $-$ are only for positive charges and negative charges; ρ is the total space charge, C·m^{-3}; φ is the potential, V; $\mathbf{j}$ is the current density, A·m^{-2}; $\mathbf{w}$ is the velocity vector, m·s^{-1}; R is the ion recombination coefficient, m^3·s^{-1}; e is the charge of the electron, 1.602×10^{-19}C; ρ is the space ionized charge density, C·m^{-3}.

To solve the ionized field, some assumptions must be introduced [5, 6]:

- The thickness of the ionization layer around the conductor is so small as to be neglected, and in other words, the research ignores the process of ionization, electron motion, etc..
- Kaptzov assumption: the magnitude of the electric field strength at the coronating conductors remains at the onset value;

$$E = E_c \tag{5}$$

  where E_c is the corona onset electric field.
- The ion mobility is independent of electric field, which means that it is constant.
- The diffusion of ions is neglected because the electrical force is far stronger than diffusion.

The problem of ionized field calculation is nonlinear because of the coupling between the electric field and space charge density. This complex problem must be numerically solved except some simple structures which have an analytic solution such as coaxial cylinder and infinite parallel planes.

Since the meshless method does not require elements or meshes to solve either the distribution of electric field in the calculation of shape function or the interpolation process, this method can solve
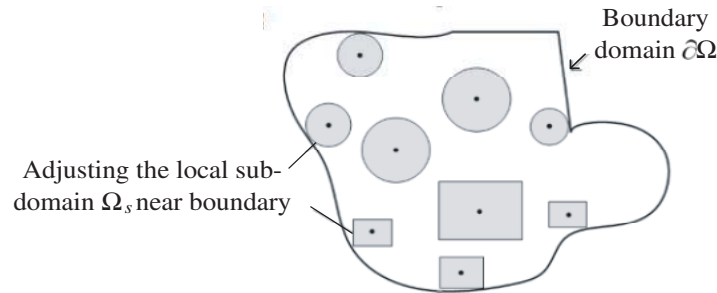

Figure 1. The local sub-domain Ωs near the global boundary have been adjusted to avoid crossing the standard limitation boundary.

the above equations efficiently. Therefore, the MLPG meshless method, which is based on the local symmetric weak form, is adopted to solve the Poisson's equations. In the paper, an improved MLPG method is proposed to calculate the ionized electric field. The local sub-domains of nodes, which are near the global boundary, have been adjusted to avoid crossing the global boundary, as shown in Figure 1. The boundary conditions including the essential and natural boundary are imposed directly by the nodes which are exactly on the global boundary based on RPIMp shape function. It is very clear that there is no boundary integration at all. Only the domain integrations over the local sub-domains are needed. As a result, the domain integrations are very easy to carry out by the improved MLPG method.

2.2. Solution of Charge Density Using Upstream Meshless Method

The nodes including m, j, and k, located in the upstream local subdomain, are selected to calculate the charge density of node i. The proposed method can capture the information from upstream, and in practice, it is found that three to six upstream nodes are good enough for the precise calculation [13, 14].

In the MLPG meshless method, the charge density of the local subdomain can be obtained as follows:

$$\rho(x) = \sum_{I}^{n} \Phi_I(x)\rho_I \tag{6}$$

where n is the number of nodes in the local subdomain, Φ_I the shape function corresponding to the node, and the RPIMp method is applied.

According to the basic equation, we can have

$$\frac{K}{\varepsilon_0}\rho^2 + \nabla\rho \cdot \mathbf{V} = 0 \tag{7}$$

where $\mathbf{V} = K\mathbf{E} + \mathbf{w}$ is the migration velocity of ions.

Inserting Equation (7) into Equations (3)~(4) will result in:

$$\frac{K}{\varepsilon_0}\rho_i^2 + (N_{I,x}(\mathbf{x})V_{ix} + N_{I,y}(\mathbf{x})V_{iy})\rho_i + \sum_{I \neq i}^{n} (N_{I,x}(\mathbf{x})\rho_I \cdot V_{ix} + N_{I,y}(\mathbf{x})\rho_I \cdot V_{iy}) = 0 \tag{8}$$

Firstly, the charge density on the surface of the conductors should be set with an initial value. The binary linear equation of the charge density is outward calculated from the surface of the conductors, and the space charge density of the whole field can be obtained.

2.3. Iteration for Ionized Field Solving

Since the space charge and electric field are coupled, we choose to apply an iterative algorithm to solve the system of Eqs. (1)–(8). The criterions of ionized electric field calculation are listed as follows:

$$\delta_\rho = |\rho_n - \rho_{n-1}| / \rho_{n-1} \tag{9}$$
$$\delta_E = |E_{\max} - E_{on}| / E_{on} \tag{10}$$

where ρ_n and ρ_{n-1} are the nth and $n-1$th calculated surface charge densities of conductor, and $E_{\max}$ is the maximum electric field of conductor surface. During the iterative calculation process, the surface density of conductor has to be updated, which can be expressed as:

$$\rho_n = \rho_{n-1}[1 + \mu(E_{\max} - E_{on})/(E_{\max} + E_{on})] \tag{11}$$

where ρ_n and ρ_{n-1} are the nth and $n-1$th calculated surface charge densities of conductor, and μ is the correctness coefficient, which is 0.6.

The ionized field can be obtained by separately solving the electric field around the conductors and the surrounding charge density. The details of the process are listed as follows:

Step I: Computing the electric field with the absence of space charge via MLPG method.

Step II: Setting an initial value of charge density on the surface of the conductors, and utilizing the upstream MLPG method to compute the space charge density based on the electric field in the step I.

Step III: Substituting charge density obtained in step II to the Poisson equation, and recalculating the electric field.

Step IV: Returning to the step II, according to the difference between the calculated electric field strength on the surface of the conductors and the corona onset electric field to update the charge density on the surface of the conductors. This will cycle until the difference between the calculated electric field strength on the surface of the conductors and the corona onset electric field δ_E to meet the error requirements, and the difference δ_p between the charge density calculated in last iteration and that value in this iteration satisfies the error requirements.
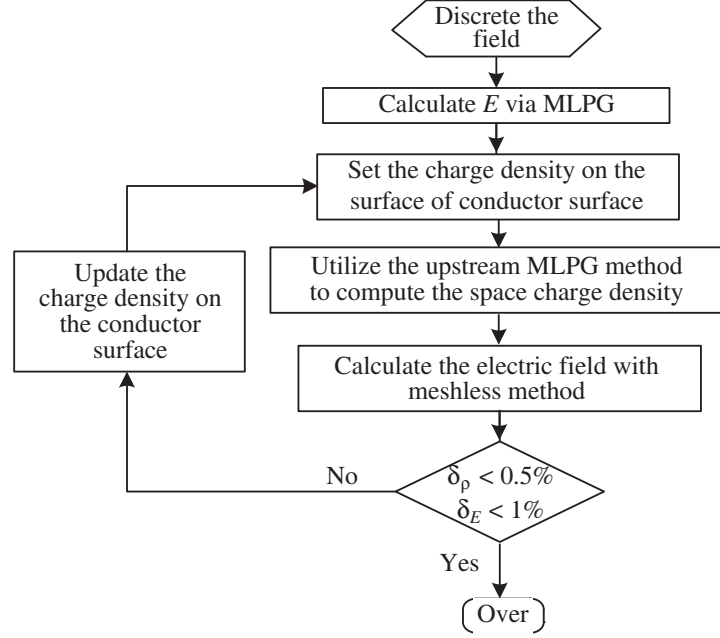
The calculation process is shown in Figure 2.

Figure 2. The calculation process for ionized field.

2.4. Validation of This Proposed Method Example Calculation

2.4.1. Coaxial Cylinder Case

To verify the validation of the proposed method in ionized field calculation, an example of high voltage transmission line is calculated using the improved MLPG method and the finite element method (FEM). The ionized field of coaxial cylinder has an analytic solution, which can be used for verification of the algorithm. Ref. [5] gives details of its solving method and results. In this paper, the ionized field of the model depicted in Figure 2 is calculated. The diameter of the inner conductor is 2 mm, and the diameter of the outer conductor is 40 mm. A voltage of 25 kV is applied on the inner conductor, and the outer conductor is grounded. The corona onset electric field is 58 kV/cm.

Figures 3(a) and (b) show the comparison of the electric field and charge density respectively. According to these results, the precision of the MLPG method used in this paper is favorable.

2.4.2. Unipolar Transmission Line

Hara and his partners [14] make a long-lasting measurement of HVDC transmission lines, and they obtain many detailed data. They use a model which has a conductor at a height of 2 m. The radius of the conductor is 0.25 cm. The corona onset electric field is 45.05 kV/cm. For this test line, [15] gives the numerical solution via FEM. In this paper, the ionized field of this test line is calculated by applying the MLPG method. The following Figures 4 and 5 show the comparison among the MLPG, FEM, and
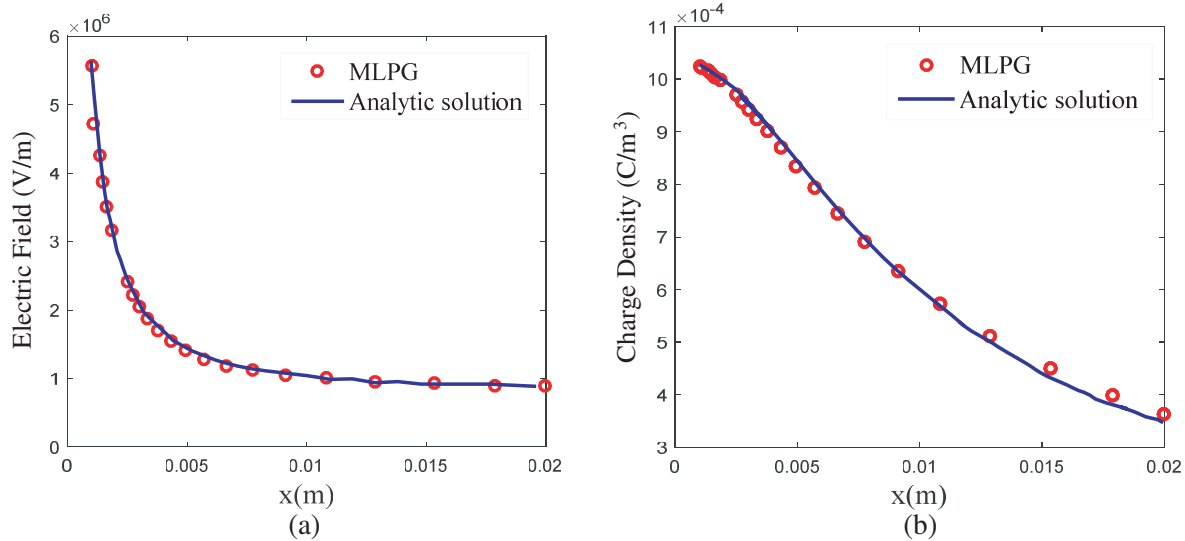
Figure 3. Comparison between the analytic solution and MLPG of the electric field and charge density. (a) Electric field, (b) charge density.
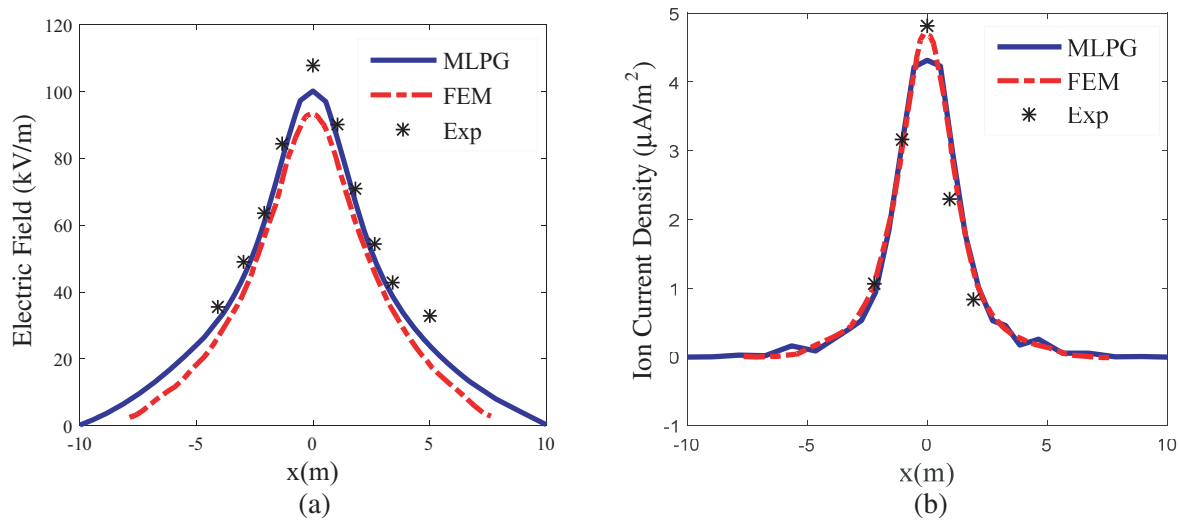

Figure 4. Comparison between the measured, FEM, and MLPG method of electric field and ion current density at ground level of the test line. (a) Electric field, (b) ion current density.

experimental data of the electric field and charge density, respectively. It can be seen that the three kinds of results agree well. There is a little difference between the MLPG and FEM results, which is caused by the precision of the algorithms. Compared to the measurement results, both MLPG and FEM results have some errors. However, the MLPG has smaller difference from experimental results than FEM method. The MLPG results coincide well with measured data.

3. INFLUENCES OF SUSPENDED PARTICLES

In practical terms, there will be a lot of suspended particles in the air because of the industrial pollution and environment deterioration. The suspended particles will charge in the ionized field, so the impact of suspended particles on the ionized field cannot be ignored.
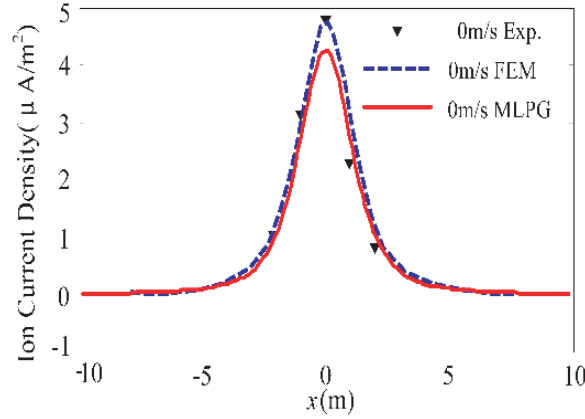
Figure 5. Comparison between the measured, FEM and meshless method of ion current at ground-level.

3.1. Charging Model of Suspended Particles

There are two ways that the suspended particles charge in the electric field: The first called electric charging is caused by the collision between the ions and suspended particles under the impact of electric force. For the particles with sizes greater than $1\,\mu m$, the electric charging plays a major role. The second called diffusion charging is caused by the diffusion of ions. This process mainly occurs on the particles with sizes less than $0.2\,\mu m$. These two processes must be simultaneously considered for the particles with the size between the two [16, 17]. The particle size of $2.5\,\mu m$ is taken as an example in this paper.

For the suspended particles in the air, the following assumptions are presented:

- The shape of the particles is standard sphere, and the particles are with the nature of uniform;
- The electric fields of the particles do not affect each other, and the particles with the same sizes can get the same charge;
- The applied electric field has local uniformity.

Figure 6 shows the geometry model of the suspended particles, and the potential of a suspended particle satisfies the Poisson equation:

$$\frac{1}{r^2}\frac{\partial}{\partial r}\left(r^2\frac{\partial u}{\partial r}\right) + \frac{1}{r^2\sin\theta}\frac{\partial}{\partial\theta}\left(\sin\theta\frac{\partial u}{\partial\theta}\right) = -\frac{\rho}{\varepsilon} \tag{12}$$

where u is potential, and ρ is the charge density of the charged particles.

The boundary conditions are as follows, and subscripts 1, 2 indicate areas 1, 2, respectively:

- At $r = 0$, the potential has a finite value $u = C$ (C is a finite real value).
- Boundary interface condition: The normal component of the electric displacement vectors are equal on the interface of the particles and the air, $\varepsilon_r\varepsilon_0 E_{1r} = \varepsilon_0 E_{2r}$. ε_r is relative dielectric constant. For suspended particles, it is 8 in this paper.
- The potential is continuous on the interface, $u_1 = u_2$.
- The synthetic electric field is equal to the applied electric in the infinite region, $E_{2r} = E_0\cos\theta$.

Substituting the equation $u = f(r)\cos\theta$ into the Poisson equation, the equations for general solutions in areas 1 and 2 are as follows:

$$r^2 f_1''(r) + 2r f_1'(r) - 2f_1(r) = 0 \tag{13}$$
$$r^2 f_2''(r) + 2r f_2'(r) - 2f_2(r) = 0 \tag{14}$$

These are Euler differential equations, and they can be solved via the conversion of $r = e^\tau$ or $\tau = \ln r$:

$$u_{21} = -E_0 r\cos\theta + \frac{\varepsilon_r - 1}{\varepsilon_r + 2}\frac{E_0 a^3}{r^2}\cos\theta \tag{15}$$
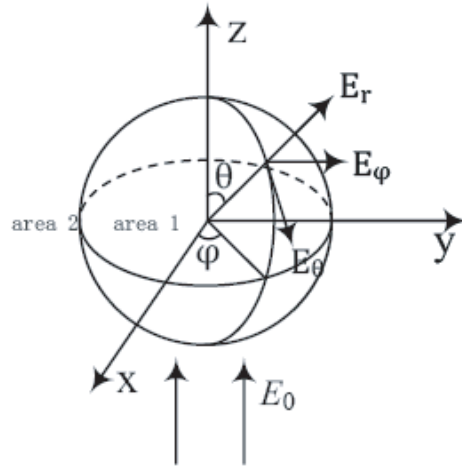
Figure 6. The geometry model of the suspended particles.

To solve the particular solution of the Poisson equation, the following equation is deduced by integral the Poisson equation:

$$\int \nabla \cdot E dV = \frac{1}{\varepsilon} \int \rho dV \tag{16}$$

Applying the Gauss divergence theorem, the particular solution can be written as follows:

$$u_{22} = \int_{\infty}^{r} \frac{q_s}{4\pi r^2 \varepsilon_0} dr \tag{17}$$

where q_s is the saturated charge.

The potential in area 2 is as follows:

$$u_2 = -E_0 r \cos \theta + \frac{\varepsilon_r - 1}{\varepsilon_r + 2} \frac{E_0 a^3}{r^2} \cos \theta + \int_{\infty}^{r} \frac{q_s}{4\pi r^2 \varepsilon_0} dr \tag{18}$$

The suspended particle is charged by the collision of the ions under the effect of electric force. With the charging of the particle, it will generate an electric field that repels the ions. The charging process completes, and the particle obtains a saturated charge when the normal component of the synthetic electric field at $\theta = \pi$ on the surface of the particle becomes zero.

$$E_r = \frac{3\varepsilon_r E_0}{\varepsilon_r + 2} - \frac{q_s}{4\pi a^2 \varepsilon_0} = 0 \tag{19}$$

So the saturated charge is obtained as:

$$q_s = \frac{12\pi a^2 \varepsilon_r \varepsilon_0 E_0}{\varepsilon_r + 2} \tag{20}$$

3.2. Influence of the Suspended Particles on Charge Density

The charged suspended particles will increase the space charge density, so the governing equations are amended as follows:

$$\nabla^2 \varphi = -\rho/\varepsilon_0 \tag{21}$$
$$\rho = \rho_e + \rho_p \tag{22}$$
$$\mathbf{j} = \rho_e (K\mathbf{E} + \mathbf{w}) \tag{23}$$
$$\nabla \cdot \mathbf{j} = 0 \tag{24}$$

where ρ_e and ρ_p are the density of ions and the charge density caused by the charged suspended particles.

The calculation process also needs to be amended as Figure 7.

In this paper, the influences of the suspended particles on the ionized field under HVDC transmission lines are discussed based on the unipolar HVDC transmission line. As an example, the density of the suspended particles is $310\,\mu g/m^3$ or 269 particles/cm^3 [18], and the size of the particle is
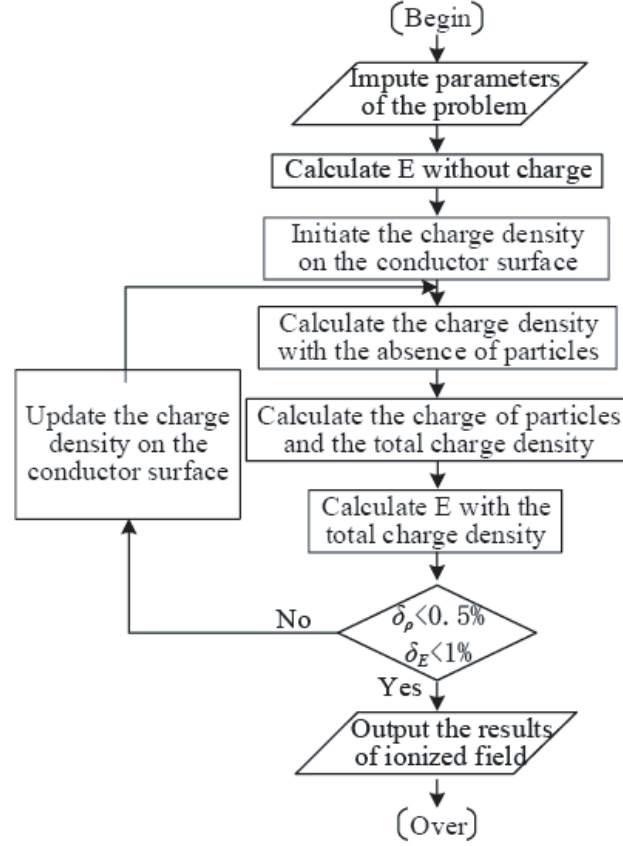

Figure 7. The calculation process with the suspended particles.
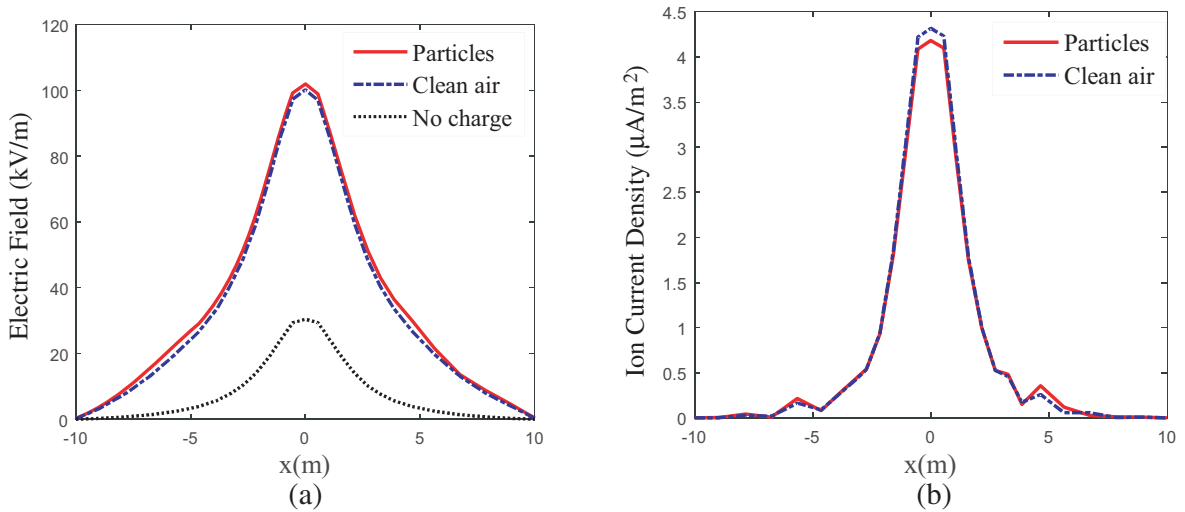

Figure 8. The electric field and ion current density at ground level with the influences of particles on space charge density only. (a) Electric field, (b) ion current density.

2.5 μm [16, 17].

Figures 8(a) and (b) show the comparison of electric field and ion current density at ground level with the influences of particles on space charge density only. In the figure, the legend "particles" represents the result with the suspended particles in the air; the legend "clean air" represents the result without suspended particles; and the legend "no charge" represents the result in charge free space. The space charge density increases because of the charging of suspended particles. Then it causes the increase of electric field strength. But the suspended particles contribute a part of the charge density, and the ion current density does not include the suspended particles. So the ion current density at ground level decreases.

3.3. Influence of Suspended Particles on Corona Onset Electric Field

The electric field strength around the conductor changes very dramatically, and suspended particles will be attracted to the conductor surface under the force of polarization. The roughness of the conductor surface is changed with this. The corona onset electric field will be reduced too. The roughness of the conductor surface usually varies between 0.4 and 0.6. In this paper, the roughness of the conductor surface is selected as 4.3 on the condition of suspended particles, and the roughness of the conductor surface is 5.0 in the clean air [19].

After the influence of suspended particles on corona onset electric field is considered, the corona onset electric field can be expressed as:

$$E'_c = \frac{m'}{m} E_c \tag{25}$$

where E'_c is the electric field strength on the conductor surface with the influence of suspended particles. m' is the roughness of the conductor surface with the influence of suspended particles. E_c is the corona onset electric field in the clean air. m is the roughness of the conductor surface in the clean air.

As shown in Figures 9(a) and (b), in the case of suspended particles, the corona onset electric field decreases. It causes the increase of the corona intensity around conductors. Then the ion current density increases too. The space charge has an effect of increase on the electric field, so the electric field strength at ground level increases.
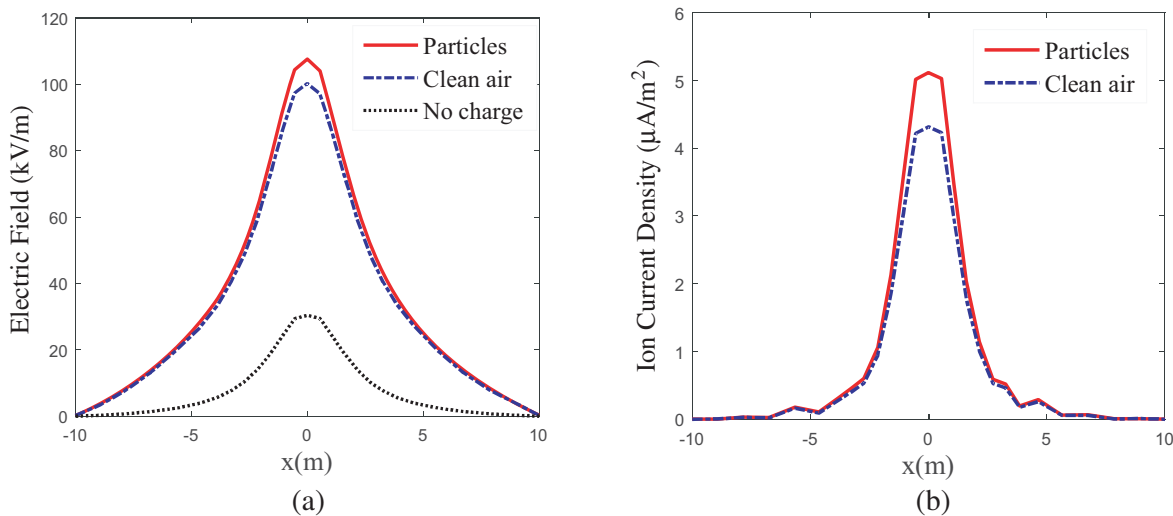

Figure 9. The electric field and ion current density at ground level with the influences of particles on corona onset electric field only. (a) Electric field, (b) ion current density.

3.4. Influence of Suspended Particles on Ion Mobility

The ion mobility with the suspended particles in air can be written as follows [20]:

$$\frac{K'}{K} = \sqrt{\frac{m_a}{m_a + m_p}} \tag{26}$$

where K is the ion mobility in the clean air. K' is the ion mobility with the suspended particles in the air. The density of the air is m_a, and the density of the suspended particles is m_p. In this paper, m_p is $310\,\mu\text{g}/\text{m}^3$.

The density of air is far bigger than the density of suspended particles in air, so as shown in Figures 10(a) and (b), the influence of suspended particles on the ion mobility is very small. The decrease of the ion mobility is less than one thousandth of itself. That is to say the ionized field is little affected by suspended particles via influence on ion mobility.
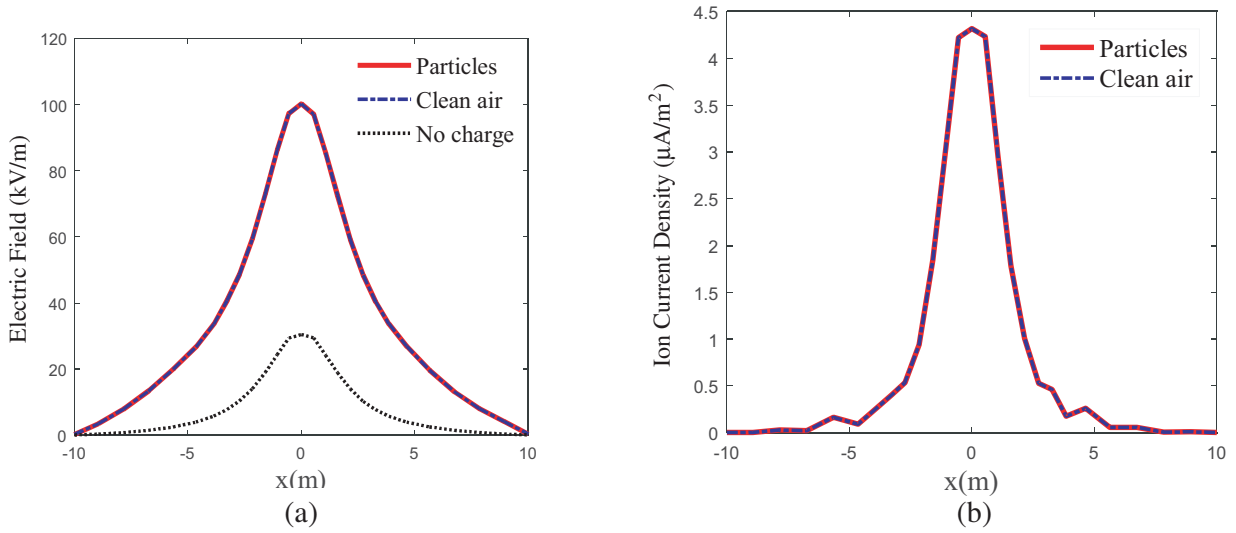

Figure 10. The electric field and ion current density at ground level with the influences of particles on the ion mobility only. (a) Electric field, (b) ion current density.

4. CONCLUSION

In this paper, the ionized field under unipolar HVDC transmission line is calculated by the improved MLPG method. It can be concluded that the MLPG method used in this paper has a favorable precision by the verification of coaxial cylinder and unipolar transmission line. On the basis of the calculated results, the influences of the suspended particles on ionized field are analyzed. The charging model of suspended particles is established by directly solving the Poisson equation. Then, the effects of suspended particles on the charge density, corona onset electric field, and ion mobility are analyzed. The study shows that the presence of charged particles will increase the space charge density, so the electric field is increased, but the ion current density is thus reduced. The suspended particles will be attracted on the conductor under the force of polarization. This will increase the roughness of the conductor surface and decrease the corona onset electric field. After the increase of the corona intensity, the ion current density and electric field will increase. The influence of suspended particles on the ion mobility is very small, so the influence of suspended particles on the ion mobility can be neglected in practical calculation.

REFERENCES

1. Li, X., I. R. Ciric, and M. R. Raghuveer, "Investigation of ionized fields due to bundled unipolar DC transmission lines in the presence of wind," *IEEE Transactions on Power Delivery*, Vol. 14, No. 1, 211–217, Jan. 1999.

2. Zhang, B., J. He, R. Zeng, S. Gu, and L. Cao, "Calculation of ion flow field under HVDC bipolar transmission lines by integral equation method," *IEEE Transactions on Magnetics*, Vol. 43, No. 4, 1237–1240, Apr. 2007.

3. Li, W., B. Zhang, J. He, R. Zeng, and S. Chen, "Research on calculation method of ion flow field under multi-circuit HVDC transmission lines," *Proc. 20th Int. Zurich Symp. Electromagn. Compat.*, 133–136, 2009.

4. He, W., Z. H. Liu, R. K. Gordon, W. E. Hutchcraft, F. Yang, and A. Chang, "A comparison of the element free Galerkin method and the meshless local Petrov-Galerkin method for solving electromagnetic problems," *Applied Computational Electromagnetics Society Journal*, Vol. 27, No. 8, 620–629, Aug. 2012.

5. Janischewskyj, W. and G. Gela, "Finite element solution for electric fields of coronating DC transmission lines," *IEEE Transactions on Power Apparatus and Systems*, Vol. 98, No. 3, 1000–1012, 1979.

6. Takuma, T., T. Ikeda, and T. Kawamoto, "Calculation of ion flow fields of HVDC transmission lines by the finite element method," *IEEE Transactions on Power Apparatus and Systems*, Vol. 100, No. 12, 4802–4810, 1981.

7. Liu, Z., W. He, F. Yang, et al., "A simple and efficient local Petrov-Galerkin meshless method and its application," *International Journal of Applied Electromagnetics and Mechanics*, Vol. 44, No. 1, 115–123, 2014.

8. He, W., Z. Liu, W. E. Hutchcraft, et al., "Complex problem domain based local Petrov-Galerkin meshless method for electromagnetic problems," *International Journal of Applied Electromagnetics and Mechanics*, Vol. 42, No. 1, 73–83, 2013.

9. F Viana S. A., D. Rodger, and H. C. Lai, "Meshless local Petrov-Galerkin method with radial basis functions applied to electromagnetics," *IEE Proceedings — Science, Measurement and Technology*, Vol. 151, No. 6, 449–451, 2004.

10. Yang, F., Z. Liu, H. Luo, X. Liu, and W. He, "Calculation of ionized field of HVDC transmission lines by the Meshless method," *IEEE Transactions on Magnetics*, Vol. 50, No. 7, Art. No. 7200406, Jul. 2014.

11. Lu, T. B., H. Feng, X. A. Cui, Z. B. Zhao, and L. Li, "Analysis of the ionized field under HVDC transmission lines in the presence of wind based on upstream finite element method," *IEEE Transactions on Magnetics*, Vol. 46, No. 8, 2939–2942, Aug. 2010.

12. Yu, M. and E. Kuffel, "A new algorithm for evaluating the fields associated with HVDC power transmission lines in the presence of Corona and strong wind," *IEEE Transactions on Magnetics*, Vol. 29, No. 2, 1985–1988, Mar. 1993.

13. Liu, Z., M. Lu, Q. Lia, et al., "Direct coupling method of meshless local Petrov-Galerkin (MLPG) and finite element method (FEM)," *International Journal of Applied Electromagnetics and Mechanics*, Vol. 51, No. 1, 51–59, 2016.

14. Hara, M., N. Hayashi, K. Shiotsuki, and M. Akazaki, "Influence of wind and conductor potential on distributions of electric field and ion current density at ground level in DC high voltage line to plane geometry," *IEEE Transactions on Power Apparatus and Systems*, Vol. 101, No. 4, 803–814, 1982.

15. Huang, G. D., J. J. Ruan, Z. Y. Du, and C. W. Zhao, "Highly stable upwind FEM for solving ionized field of HVDC transmission line," *IEEE Transactions on Magnetics*, Vol. 48, No. 2, 719–722, Feb. 2012.

16. White, H. J., "Particle changing in electrostatic precipitation," *AIEE Transactions*, Vol. 70, 1186–1191, 1951.

17. Kim, K. B. and B. J. Yoon, "Field charging of spherical particles in linear electric field," *Journal of Colloid & Interface Science*, Vol. 186, No. 1, 209–211, 1997.

18. Liu, H. L., "Research on measurement method of the concentration and size distribution of indoor suspended particulate matters," Huazhong University of Science and Technology, 2009.

19. Zhao, Y. S. and W. L. Zhang, "Effects of fog on ion flow field under HVDC transmission lines," *Proceedings of the CSEE*, Vol. 33, No. 13, 194–199, May 2013.

20. Tan, Z. N., J. H. Yang, M. M. Xu, et al., "Influence of Fog-Haze on corona ion flow field of HVDC transmission lines," *High Voltage Engineering*, Vol. 42, No. 12, 3844–3852, Dec. 2016.